

## OPTICAL FOLLOW-UP OF THE REFLEX SURVEY: A NEW PERSPECTIVE IN CLUSTER STUDIES

L.T. BARONE<sup>1,2</sup>, E. MOLINARI<sup>2</sup>, H. BÖHRINGER<sup>3</sup>, G. CHINCARINI<sup>2</sup>, C.A. COLLINS<sup>4</sup>, L. GUZZO<sup>2</sup>, P.D. LYNAM<sup>3</sup>, D.M. NEUMANN<sup>5</sup>, T. REIPRICH<sup>3</sup>, S. SCHINDLER<sup>4</sup>, P. SCHUECKER<sup>3</sup>

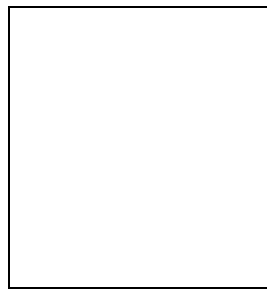
<sup>1</sup> *Università degli Studi di Milano, Dipartimento di Fisica, Via Celoria 16, 20133 Milano, Italy*

<sup>2</sup> *Osservatorio Astronomico di Brera, Via E. Bianchi 46, 23807 Merate (LC), Italy*

<sup>3</sup> *Max-Planck-Institut für extraterrestrische Physik, Giessenbachstr. 1, 85740 Garching, Germany*

<sup>4</sup> *Liverpool John Moores University, Birkenhead, L41 1LD, U.K.*

<sup>5</sup> *CEA/Saclay, L'Orme des Merisiers, 91191 Gif-sur-Yvette, France*



After the completion of the catalogue built with ESO key program (REFLEX), we are beginning to explore the multiband optical characteristics of a subsample of those clusters selected in a statistically independent way. We have already observed in B, V, R, 9 of the about 50 clusters of the subsample, with  $0.15 \leq z \leq 0.18$ . More time has been allocated by ESO for our project in March 2001. We will therefore be able to compare X-ray and optical morphologies and luminosities and, thanks to the large field of view of the WFI instrument, assess the luminosity function and the color segregation in the cluster on a robust statistical basis. In this poster we present the project, the technical problems we are facing in the reduction phase, and show the first preliminary results, which seem very encouraging.

### 1 Introduction

The study of individual cluster of galaxies can be considered as the repetition of the same experiment, conducted under varying sets of initial conditions. Unfortunately, the observer only has a comparatively poor knowledge of the 'exact' initial conditions in each cluster/experiment. As the intrinsic and environmental conditions cannot be chosen, a statistical approach is the only effective one in a proper attempt to extract the rules of the experiment, as it is very frequently the case in astronomy.

The problem of robust statistical sample selection of galaxy clusters has always been a concern, and only with X-ray astronomy — a tool which is more objective than optical identification

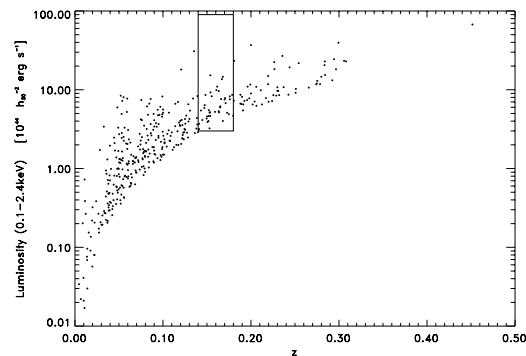


Figure 1: Optical subsample of the REFLEX cluster survey. The rectangle indicates the clusters belonging to the subsample objective of our study, with redshifts  $0.15 \leq z \leq 0.18$ .

— at astronomers' disposal can such a selection be reliably performed. Furthermore, the X-ray luminosity offers an indirect but reliable estimate of the gravitational mass of the whole cluster as shown by the tight relation of the two cluster properties in recent work by Reiprich & Böhringer<sup>7</sup>.

The cluster characteristics observed in the optical band are the goal of the present project and will be analyzed and catalogued as a function of the main X-ray properties.

### 1.1 The REFLEX sample

A unique opportunity in this sense is provided by the recent completion of the ESO key programme (REFLEX) aimed at the redshift measurement of all the candidate clusters selected in the ROSAT All Sky Survey (RASS) in the Southern Hemisphere. This programme (Böhringer *et al.*<sup>2</sup>, Guzzo *et al.*<sup>4</sup>, De Grandi *et al.*<sup>3</sup>) produced a well-controlled sample of 452 galaxy clusters down to a flux limit of  $3 \times 10^{-12}$  erg sec<sup>-1</sup> cm<sup>-2</sup>. Its X-ray luminosity *vs.* redshift distribution is reported in Fig. 1.

### 1.2 The subsample

A REFLEX subsample of about 50 clusters (Fig. 2) with redshift around 0.15 (Fig. 3) has thus been selected to begin an optical follow-up campaign in the three bands B, V, R. Nine out of these 50 clusters have already been observed in two different observation runs in the years 1999

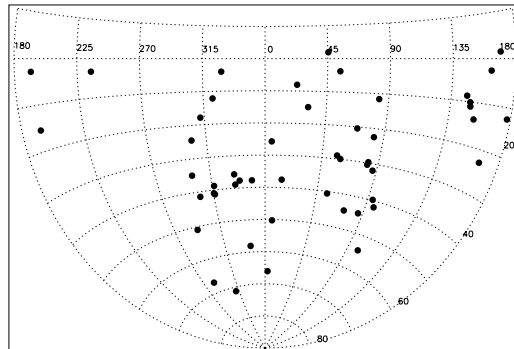


Figure 2: Distribution on the Southern Hemisphere of the REFLEX subsample.

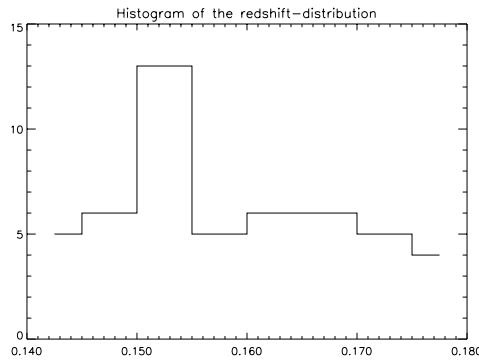


Figure 3: Redshift distribution of the subsample.

and 2000 at the 2.2-m ESO Telescope in La Silla (Chile). Three more nights have been allocated for this project in March 2001.

The instrument used for this study is the WFI (Wide Field Imager), which is a mosaic made of 8 CCDs to cover a total field of about  $30' \times 30'$  (about  $8000 \times 8000$  pxl). At redshift 0.15, this corresponds to a field of  $5 \times 5$  Mpc<sup>2</sup> for each telescope pointing. This field is therefore ideal to best cover all the typical virial radii of clusters ( $\sim 3h_{50}^{-1}$  Mpc) and to analyze cluster properties on scales far from the centre. With the exposure times used, the limit magnitude in V is about 24. Figure 4 shows, for comparison, what we expect that a typical galaxy spectrum looks like at a redshift of 0.15. The bands we observed fall exactly in the right range to capture the 4000-break.

## 2 Our analysis

For the observation, we used a dithering pattern involving 6 exposures per cluster per colour which allows in the data reduction phase a reconstruction of the whole field of view with a fairly uniform exposure ( $\geq 80\%$  of the exposure time). The end product shall be deep integrations of the entire virial regions of the clusters. For the calibration of the camera, we conduct observations of standard stars for each of the chips in each colour and monitor the photometric conditions with further standard star observations during the night.

For the reduction, the IRAF package has been used. In particular, the tasks *esowfi* and

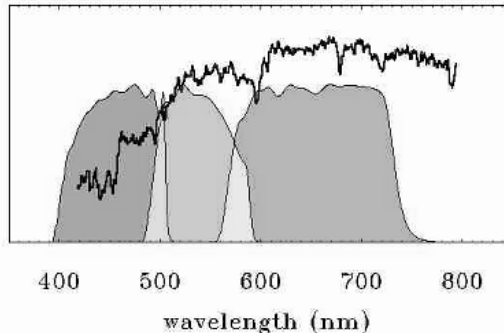


Figure 4: A typical galaxy spectrum redshifted at  $z = 0.15$ : superposed are the 3 bands we used. The galaxy is NGC 4472, from Kennicutt <sup>6</sup>.

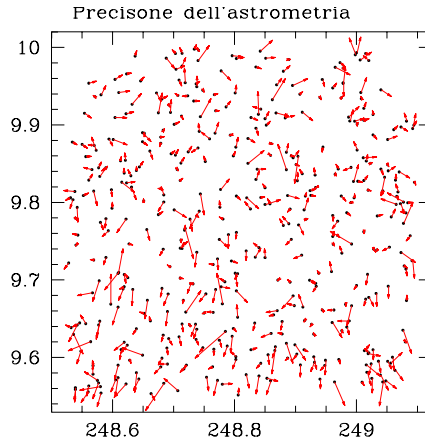


Figure 5: The astrometric correction we performed on one of our images with respect to the USNO catalogue (whose internal error is about 0.4 arcsec) freed from systemic errors. On the abscissa the alpha coordinate of the image is plotted; on the ordinate the declination is plotted. The arrows are enhanced 100 times.

*mscred* are specifically designed to face mosaic reduction of ESO WFI data.

The data reduction process (still *in fieri*) has proved particularly demanding.

### 2.1 Astrometric correction

At first, the problem of astrometric correction has to be faced. The tasks used by IRAF make use of Valdes' (1998) correction. In order to do this, the procedure we applied is the following. Given one of the images either of the 6 dithering sequence or of the standard star fields, by use of *Skycat*, it was compared with an external star catalogue (USNO). The comparison involves two steps:

1. an initial rough spatial shift on the plane, due to the fact that the center of the CCD (and of the telescope) and of Valdes' correction do not coincide and due to the telescope pointing imprecision;
2. a more precise matching, which is obtained by three corrections applied to the image: tangent point shift, fractional scale change and axis rotation.

This latter phase is obtained by IRAF by comparing the intensity peaks of the image with the given catalogue. The choice of the points to exclude from the fit is obtained by manual correction to avoid spurious "detections" and minimize the rms.

Subsequently, another catalogue is obtained with *SEXTRACTOR* (Bertin & Arnouts<sup>1</sup>) from the corrected image, which is in turn used for the other images of the sequence (of dithering images or of star fields) for the astrometric correction. Clearly, it is the correspondence with *this* internal catalogue to be important, since, once the dithered images are corrected, when they will have to be stacked, it is the *internal* precision that will affect the goodness of the final (cluster) image. This second process is analogous to the aforementioned one, except for the use of the other catalogue.

In Fig. 5 we show, as an example, the corrections applied astrometrically on one of our star field images with respect to the *external* catalogue. The final error we obtain in the comparison with the *internal* catalogue is about  $\pm 0.5$  arcsec, well within an acceptable range, considering that the error in the USNO is about 0.4 arcsec.

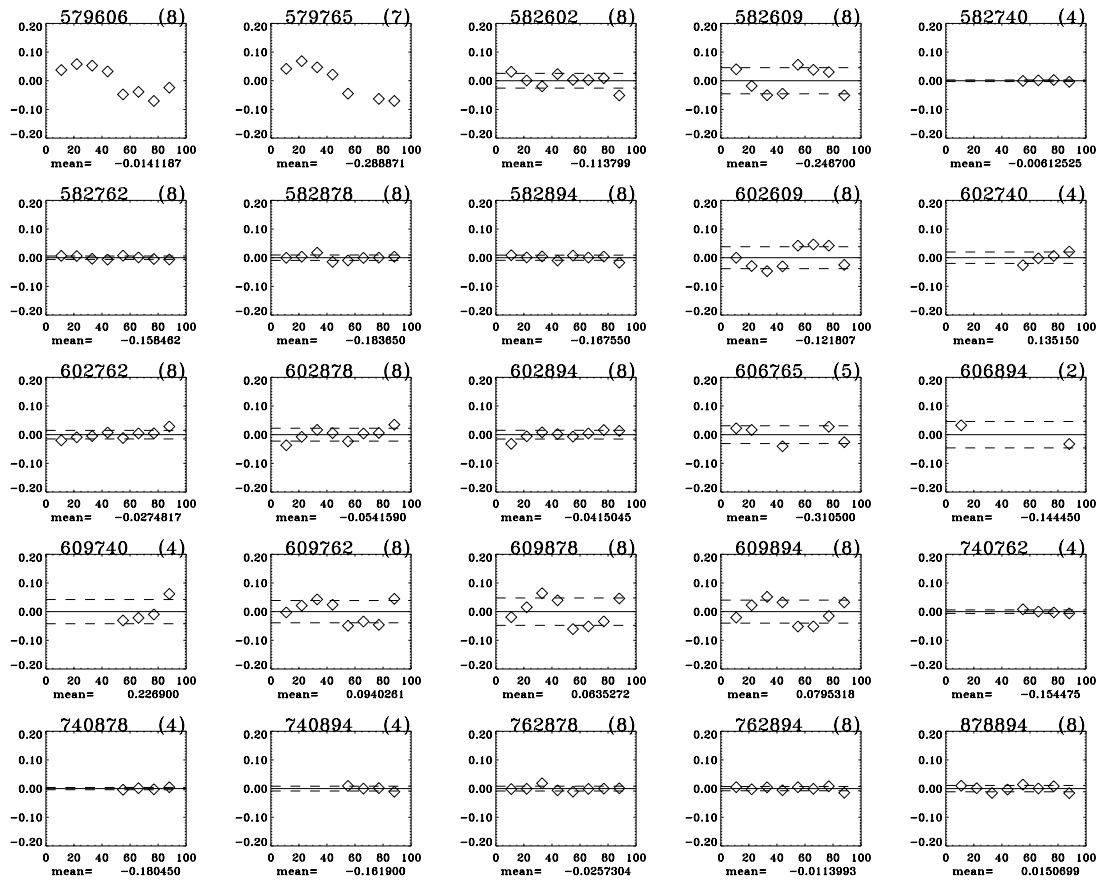


Figure 6: This figure shows the comparison between different couples of catalogues coming from different exposures of the same (stellar) fields. Once the average displacement value from 0 has been calculated (small caption beneath each plot), for each couple of catalogues for the objects present in both catalogues on the  $n$ th chip (here only the  $nm$  values are shown, on the abscissa of each plot), such value has been added to each of the value  $nm$ . In those cases when the variations were  $\leq 0.05$  mag,  $1\sigma$  dashed lines have been traced and such values have been used to calculate the reciprocal efficiency of the 2 CCDs for the  $nm$  cases, shown in Fig. 7.

## 2.2 Photometric correction

The procedure used for the subtraction of the flat field, should guarantee that the chip-to-chip variations are taken care of. In order for us to verify that this is actually the case, we developed a process that allows us to check that these originally non-negligible variations are effectively reduced.

In Fig. 6 we represent the 2-by-2 comparisons between different catalogues obtained from images of the same stellar field, for which a comparison of the objects on the  $n$ th CCD with the same  $n$ th CCD in another image is available ( $n = 1, 2, \dots, 8$ ). These values have been averaged out and normalized to 0 (the small number on the bottom of each plot indicates the averaged number that has been added to the values for this normalization). Accepted were only those  $nm$  variations  $\leq 0.05$  mag;  $1\sigma$  dashed lines have then been traced.

For those couples of catalogues for which the  $nm$  values were acceptable, the values of the calibration (excluding the normalization) for the  $nm$  CCDs (with  $n \neq m$ ) have been calculated, as shown in Fig. 7.

Finally, on Fig. 8 we sketched the numbers which need to be used to move from one chip to the other. Only one star field image sequence has been used to obtain those numbers and only one filter. Numbers still need refinement, but the results shown indicate that the flat field

subtraction seems to be sufficient to correct for the chip-to-chip variations.

### 3 Preliminary results

A preliminary Luminosity Function in V of the area of the core of cluster R1540, performed on only 1 of the 6 dithered images of the cluster (1 chip) is shown on Fig. 3. Even if the image is only a number count of the objects based on a simple *SEXTRACTOR* result (no background subtracted), it still shows an interesting trend. For comparison, we show on the right panel of Fig. 3 a figure coming from Molinari<sup>5</sup>. In the plot of the 5 low redshift clusters the bimodality separating the giant from the dwarf ellipticals is evident.

The core of cluster R1540 is the one shown in the background image of the poster presented (Fig. 11).

### Acknowledgments

We would like to thank S. Benetti and A. Zacchei (TNG staff) for help in producing the poster background image (Fig. 11) and L. Rizzi for his constant help and precious tips and suggestions in the data reduction process. We are also very grateful to A. Moretti for valuable help in the clusters observations.

### References

1. E. Bertin & S. Arnouts, *A&AS* **117**, 393B (1996).
2. H. Böhringer, Guzzo, C.A. Collins, *et al.*, proceedings of the 14th IAP Meeting *Wide Field Surveys in Cosmology*, Y.Mellier & S. Colombi (eds) , (1998), see also astro-ph/9809381.
3. S. De Grandi, H. Böhringer, L. Guzzo, *et al.*, *ApJ* **514**, 148 (1999).
4. L. Guzzo, H. Böhringer, P. Schuecker, *et al.*, *The Messenger* **95**, 27 (1999).
5. E. Molinari, proceedings of the Johannesburg Conference *Toward a New Millenium in Galaxy Morphology*, D.L. Block, I. Puerari, A. Stockton, and D. Ferreira (eds) , 685 (1999).
6. R.C. Kennicutt, Jr., *ApJS* **79**, 255K (1992).
7. T. Reiprich & H. Böhringer, *Astr. Nachr.* **320**, 296 (1999).

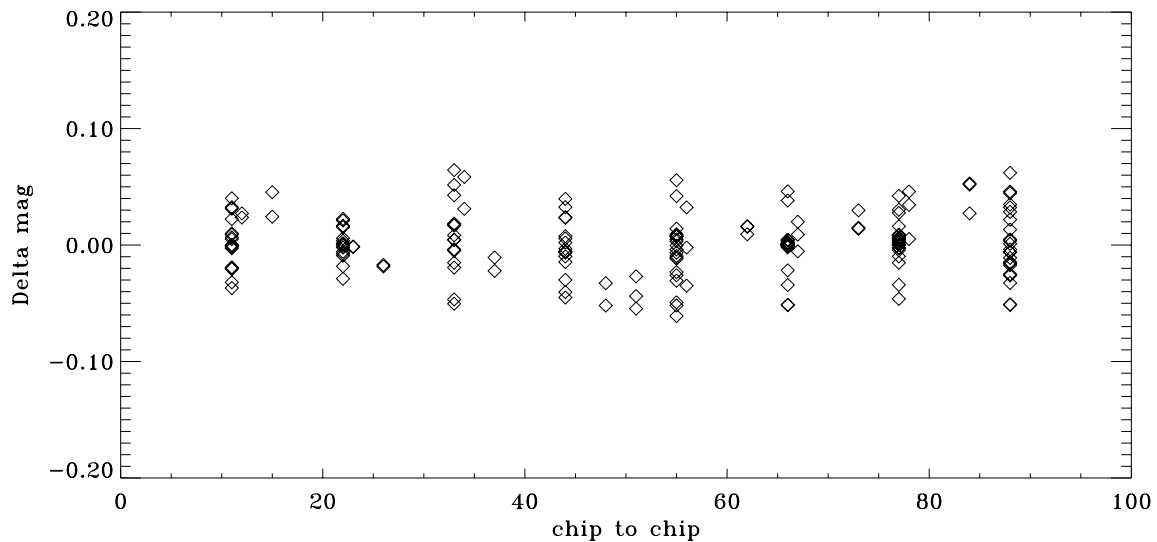


Figure 7: In this figure all the  $nm$  couples are shown, for which “accepted”  $nn$  values are available (Fig. 6)

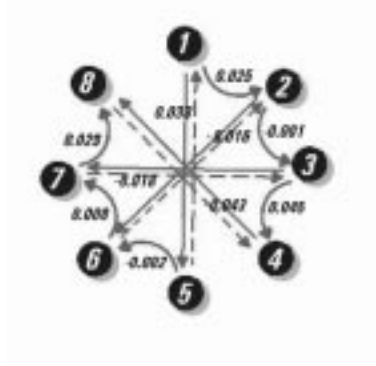


Figure 8: Resulting coefficients for the chip-to-chip calibrations. Only one star field has been used so far to produce this numbers. Calibrations still need refinement, but they already seem to show that the flat field subtraction is sufficient to take care of the chip-to-chip variations.

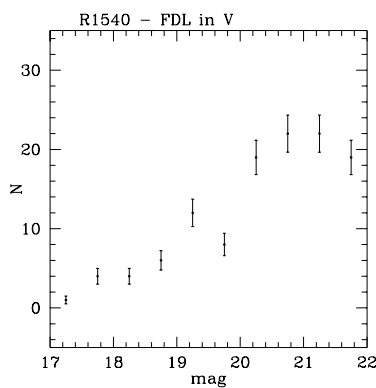


Figure 9: Number counts of the core of cluster R1540. Errors are poissonian. Bins are of 0.5 mag. Time of exposure is of the order of 7 min. For  $\text{mag} \geq 20$  clearly we begin missing something.

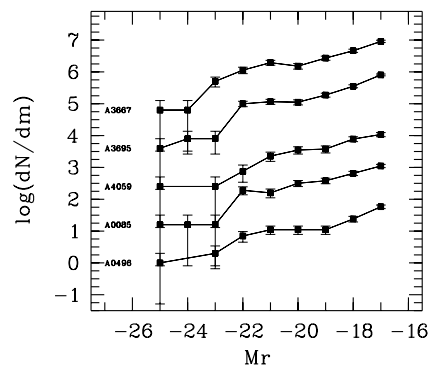


Figure 10: This image comes from Molinari <sup>5</sup> and shows the bimodality between giant and dwarf ellipticals in a sample of 5 low redshift clusters.

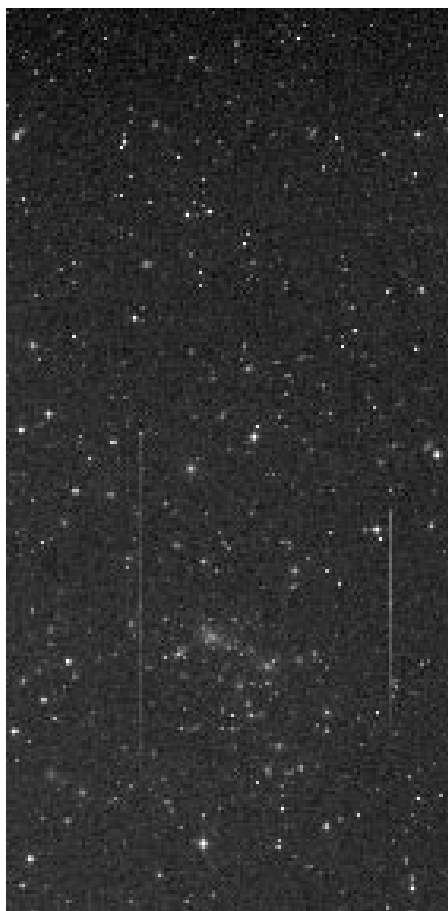


Figure 11: Background of the poster. The core of the cluster R1540. The three BVR filters have been used up to produce the image. This comes only from 1 chip and a single exposure.